Complete Bromide Surface Segregation in Mixed NaCl/NaBr Aerosols Grown from Droplets

Egill Antonsson,[1] Minna Patanen,[1] Christophe Nicolas,[1] John J. Neville,[1,2] Safia Benkoula,[1] Alok Goel,[1] and Catalin Miron[1,3,*]

[1]*Synchrotron SOLEIL, l'Orme des Merisiers, Saint-Aubin, BP 48, 91192 Gif-sur-Yvette Cedex, France*
[2]*Department of Chemistry, University of New Brunswick, Fredericton, NB E3B 5A3, Canada*
[3]*Extreme Light Infrastructure-Nuclear Physics (ELI-NP), "Horia Hulubei" National Institute for Physics and Nuclear Engineering, 30 Reactorului Street, RO-077125 Măgurele, Judeţul Ilfov, Romania*

(Received 26 August 2014; published 3 March 2015)

Sea-salt aerosols are a source of atmospheric bromine responsible for ozone depletion. The availability of bromine from sea-salt aerosols to heterogeneous phase chemical reactions is determined by its local concentration at the aerosol surface. We report here complete surface segregation of bromine in mixed NaCl/NaBr aerosols grown by drying droplets, thus mimicking the atmospheric process by which solid sea-salt aerosols are generated. For $d = 70$ nm solid aerosols, complete surface segregation is observed for solution Br/Cl ratios below 2%. These findings set a size-dependent upper limit on the bromine surface enrichment that can be reached in solid salt aerosols grown from sea-water droplets in the atmosphere.

DOI: 10.1103/PhysRevX.5.011025

Subject Areas: Atomic and Molecular Physics, Nanophysics, Physical Chemistry

I. INTRODUCTION

Sea-salt aerosols are among the most abundant aerosols in the atmosphere. In addition to their role in past [1] and present [2] climate change, they play a crucial role in ozone depletion. During the arctic sunrise in the spring, near-complete ozone depletion coincides with a rise in concentration of bromine-containing compounds [3–5]. Evidence points to sea salt as being an important source of the bromine [6], both as aerosols and deposited on snow [7,8]. Mechanisms have been proposed for both the halogen release from sea-salt aerosols [9] and for the halogen-catalyzed reactions leading to ozone depletion [10]. The kinetics of halogen reactions at the aerosol surface depend critically on the relative amount of Cl and Br at the surface [4] since the surface composition dictates which species are available to chemically react with the surrounding gas phase. This motivates the interest in understanding the local surface composition of sea-salt aerosols as opposed to their bulk composition. The bromine/chlorine ratio in sea-water is 1:660 (0.15%) [11], and in the absence of surface segregation, the same value is also expected at the surface of sea-salt aerosols. Sea-salt aerosols are formed from sea-spray droplets after water evaporation, and they exist in air as liquid drops, deliquescent drops, or as dry sea-salt particles depending on the relative humidity of the surroundings [12]. For NaCl, the most abundant salt in sea water, the efflorescence point lies at 45% relative humidity while showing some dependence on the size of the particles [13]. Sea-salt aerosols exist in a wide size distribution ranging from ultrafine particles of diameters down to 5 nm, up to particles in the micron size range [14]. Their size critically influences their lifetime in the atmosphere, the smaller aerosols being likelier to leave the humid oceanic regions and be transported by wind to dryer regions where they can crystallize to form solids. High-altitude measurements of aerosol concentration above the Pacific Ocean show an increase in particle-number density in the nanometer-size range [15]. For particles that reside long in the atmosphere, the size distribution becomes skewed towards smaller particles, as larger particles are removed by gravitational settling [16]. This motivates the interest in studying finite-size aerosols grown from water solution droplets, as opposed to quasi-infinite-size bulk-model systems.

The surface composition in solid sea-salt aerosols reflects both the structure of the precursor droplets and the dynamics of the evaporation/crystallization process. A paradigm shift in our understanding of local ion concentration in aqueous solutions has occurred in the last 10 to 15 years, whereby the previous model of a water-gas interface devoid of ions has been replaced with a model, supported by both experimental and theoretical evidence, where ions can lie at the surface and even be enriched at the surface as compared to the bulk [17–19].

Previous studies of NaCl/NaBr binary bulk crystals grown from solutions have revealed up to 35-fold [20] surface enhancement of bromine over the average concentration in the crystals as a whole. Similarly, a 38-fold

*Corresponding author.
Catalin.Miron@synchrotron-soleil.fr

concentration increase at the surface was observed when sea-water aerosols in the size range of around 10 μm were deposited on ice packs [21]. Furthermore, studies on wetted, macroscopic NaCl/NaBr mixed crystals have explored the halogen ion ratios at the surface and revealed an excess of surface bromide [22]. Surface enhancement of bromine in atmospherically relevant aerosols in the nanometer size range has not yet been studied. In contrast to the above studies, which model the chemistry of micron-size deposited salt particles, here we address the important issue of bromine surface segregation from a different viewpoint more relevant to the way sea-salt aerosols are generated in the atmosphere. Our data undoubtedly demonstrate that complete bromine surface segregation takes place in submicron solid aerosols. Here, complete surface segregation means that all bromine ions contained in the initial droplets end up in the thin surface layer of the solid aerosols that is probed by electron spectroscopy. We show that the finite amount of bromine in such aerosols and their high surface/bulk ratio set an upper limit to the surface enrichment.

II. EXPERIMENTAL

NaCl and NaBr salts ($\geq$ 99.99% purity, Sigma Aldrich) were dissolved in water purified with a milli-Q system (Millipore, Saint-Quentin en Yvelines, France). The purified water has a stated total-organic-carbon content of < 5 ppb (μg/L), orders of magnitude lower than the salt-solution concentration, ensuring a very low risk of carbon contamination of the sample. The solutions were sprayed into a nitrogen atmosphere using a commercial atomizer [Model 3076, TSI (Shoreview, MN)], which generates droplets that are dried using two silica gel diffusion dryers (Model 3062, TSI), yielding solid aerosols of mixed alkali halides. The obtained size distribution from a 1% NaBr/NaCl aqueous solution as determined with a differential mobility analyzer coupled to a condensation particle counter is shown in Fig. 1(a) and revealed a log-normal size distribution with the mode of the distribution at $d = 70$ nm. Other mixing ratios of NaBr and NaCl did not result in significantly different size distributions. The resulting alkali halide nanoscale aerosols are transferred into vacuum and focused with an aerodynamic lens system [23–28], which yields a collimated beam of isolated aerosols with a full-width-at-half-maximum of 550 μm. The profile of the aerosol beam is shown in Fig. 1(b). It was obtained by recording the total electron yield from $d = 70$-nm NaCl aerosols while moving the outlet of the aerodynamic lens system relative to the x-ray beam. The background pressure in the interaction chamber was typically 10^{-6} mbar during the experiments.

The probed depth in x-ray photoelectron spectroscopy is considered to be 3 times the inelastic mean-free path of the photoelectrons [29]. Using a photon energy of 133.5 eV, we estimate the inelastic mean-free path for Br 3d and Na 2s photoelectrons to be 0.60 nm and 0.62 nm, respectively [30]. The photoelectrons' escape depth is thus around 2 nm.

The experiments were performed at the SOLEIL synchrotron radiation facility (Saint-Aubin, France) at the PLEIADES beam line [31], which is dedicated to soft x-ray spectroscopy studies of dilute samples ranging in size from atoms [32] and molecules [33–36] to clusters [37] and nanoparticles [24,38,39]. The polarization vector of the radiation was chosen to be parallel to the spectrometer axis. The bandwidth of the x rays was set to 127 meV. The photoelectron spectra were recorded with a VG-Scienta R4000 electron spectrometer operated with a pass energy of 200 eV and an entrance slit opening of 800 μm, resulting in a spectrometer resolution of 400 meV and an overall experimental resolution of 420 meV.

III. RESULTS AND DISCUSSION

Photoelectron spectra of mixed NaCl/NaBr solid nanoscale aerosols with variable salt mixing ratios in the primary droplets are presented in Fig. 2. The features associated with emission of localized Br 3d and Na 2s electrons are marked on the figure. The observed rise in

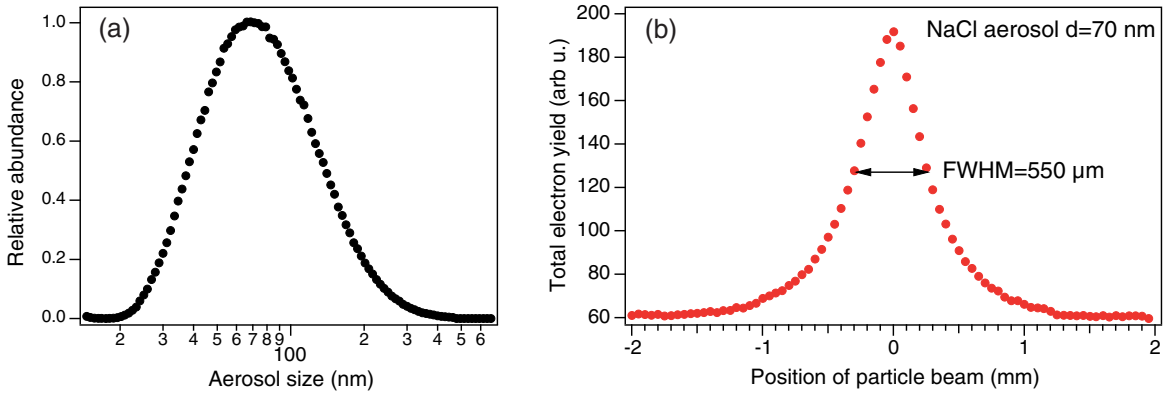

FIG. 1. (a) Aerosol-size distribution after spraying of a 1 g/L 1% NaBr/NaCl solution and subsequent drying. (b) Total electron yield from $d = 70$-nm aerosol ionized with a photon energy of 100 eV while moving the outlet of the aerodynamic lens system. The aerosol beam is found to have a full-width-at-half maximum of 550 μm.

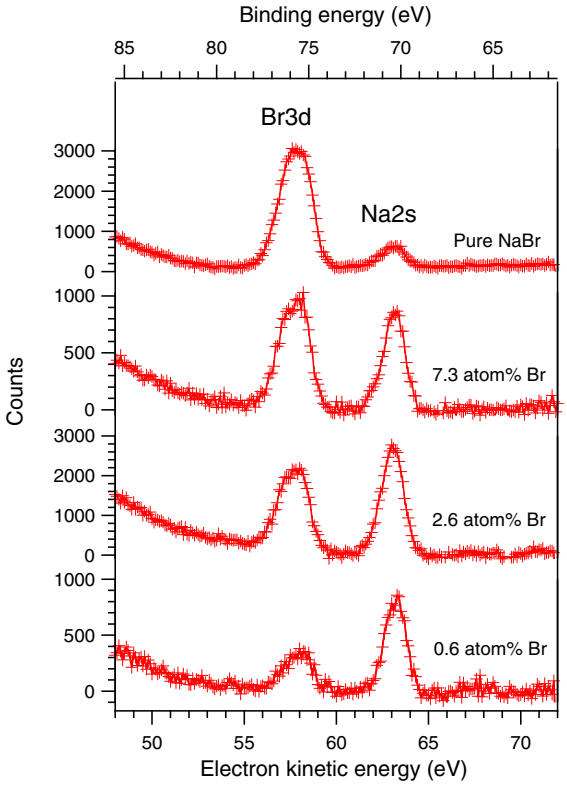

FIG. 2. Photoelectron spectra of mixed NaCl/NaBr solid aerosols generated from solution droplets with different NaCl/NaBr mixing ratios. The Br/Cl ion ratio in the solution is indicated for each spectrum. By using the Br 3d/Na 2s ratio in pure NaBr aerosols, the Br/Cl surface ratio in the mixed solid aerosols is inferred. The spectra have been recorded at a photon energy of 133.5 eV, which generates photoelectrons with kinetic energies lying at the minimum of the "universal curve" of the electron inelastic mean-free-path to ensure maximum surface sensitivity. The acquisition time for each spectrum is around two hours.

electron signal at low kinetic energy is due to inelastic scattering of the outgoing photoelectrons. For comparison, a similar photoelectron spectrum of pure NaBr aerosols is also shown. For each of the spectra in Fig. 2, the acquisition time is around two hours.

The photon energy used in the experiments was 133.5 eV, which led to electron kinetic energies lying close to the minimum of the "universal curve" [30] for the electron inelastic mean-free path in the aerosols, which confers maximal surface sensitivity to the experiments. Because of the reduced inelastic mean-free path of the photoelectrons in the solid particles, the spectra in Fig. 2 only reflect the particle composition in the topmost 2 nm of the particles, photoelectrons originating from deeper regions in the aerosols not being able to reach the surface. The simultaneous measurement of the Br 3d and Na 2s lines eliminates the need for normalization with respect to photon flux and particle density and prevents the need for assumptions about photoabsorption cross sections and photoemission angular anisotropy.

When increasing the amount of NaBr relative to NaCl in the primary droplets, the Br 3d photoemission signal increases relative to the Na 2s signal, which is interpreted as an increase of the Br content at the surface. The Br 3d signal acts as a gauge of the Br/Cl surface concentration since a rise in the Br surface concentration corresponds to a drop in the Cl concentration to maintain charge neutrality. For the same reason, the amount of Na ions in the probed region is equal to the total amount of anions.

Under these drying conditions, the particles are found to be devoid of water. This was confirmed by x-ray absorption measurements near the O 1s absorption edge where no O 1s signal is found for any of the aerosols [40]. This important control experiment excludes the possibility that the enhanced Br 3d signal might be due to a residual water film on the surface of the aerosols, leaving only the possibility that the Br enhancement is indeed at the surface of the solid aerosols.

Figure 3(a) shows the Br 3d/Na 2s photoemission signal ratios (right axis) measured at several NaCl/NaBr mixing ratios in the precursor liquid droplets. The point at 100% Br was obtained for pure NaBr aerosols (topmost spectrum in Fig. 2). Using the Br 3d/Na 2s ratio for such pure NaBr aerosols (7.56 ± 0.41), corresponding to a 1:1 ratio of Br/Na atoms, the percentage of bromine atoms with respect to the total amount of anions within the probed surface region can be determined and is shown on the left axis. While the NaBr/NaCl is varied, the total salt concentration is kept constant at 1 g/L to ensure constant aerosol size.

As for the mixing ratios shown in Fig. 2, the bromine surface concentration for the solid aerosols exceeds that in the primary droplets and shows a pronounced dependence on the mixing ratio in the droplets. In Fig. 3(a), the measured surface concentrations of bromine are compared to three models for ion distribution in the solid aerosols: (i) The broken line with a slope of 1 corresponds to the bromine surface concentration if the bromine and chlorine ions were homogeneously distributed throughout the whole volume of the aerosol and the ratio is determined by the bromine/chlorine ratios in the primary droplets. This model underestimates the bromine surface concentration, supporting surface segregation of bromine. (ii) The dotted line shows a model of complete surface segregation, where all the Br ions contained in the primary droplets are in the surface region of the solid aerosol. For a 70-nm-diameter sphere, used as a model for the particles in the present study that have an aerodynamic diameter of 70 nm, 16% of the particle volume is contained in the outermost 2 nm, which is the depth probed in this experiment. If *all* bromine ions in the primary droplets end up in the surface layer of the solid aerosol following the evaporation of the water and crystallization of the salts, one would expect the experimental points to follow a straight line of slope 6.25, which is equal

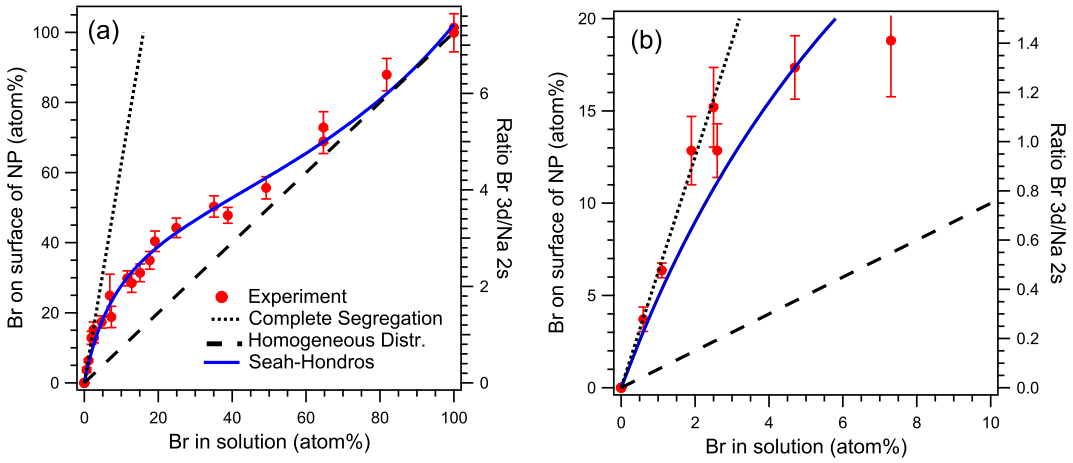

FIG. 3. Br/Cl ion surface ratios in d = 70-nm aerosols as a function of the Br/Cl atom ratio in the primary droplets. (a) Ratio of integrated Br 3d and Na 2s photoemission signals (right axis) and the resulting surface atom percentage as a function of the mixing ratio (left axis). The broken line represents a model with no surface segregation, and the dotted line represents a model with complete segregation (all bromine ions in the primary droplet end up in the surface region of the solid aerosol—see text). The blue curve is based on a fit to the Seah-Hondros theory of surface segregation. (b) Zoom-in of the low-mixing-ratio region where complete bromide surface segregation is observed.

to the volume/surface ratio. This model of complete segregation describes the experimental data well at low mixing ratios, indicating full bromine surface segregation at mixing ratios below ≈2%. This region is emphasized in Fig. 3(b), showing that complete surface segregation of bromine ions takes place. (iii) Lastly, the blue curve corresponds to a fit to the measured data using the expression for surface segregation in solids given by Seah and Hondros [41], which is a condensed-phase analogue to the gas-phase adsorption theory of Brunauer, Emmett, and Teller [42]. Here, the driving force for the segregation is the higher surface affinity of one of the two species in the binary mixture. It accounts for multilayer adsorption to an interface. In this model, the linear increase of the surface concentration at low mixing ratios is due to all surface-affine species (bromine in this case) finding a spot on the surface, whereas the later leveling off is a consequence of partial surface coverage and competition between bromine ions for the finite number of available surface spots. This is due to the surface affinity of the first layer being greater than that of subsequent layers.

The surface enhancement phenomenon observed in the mixed NaBr/NaCl aerosols is illustrated in Fig. 4 as the measured ion surface concentration in the solid aerosols compared to the concentration in the primary droplets. The horizontal full and dash-dotted lines indicate the maximal bromine surface enrichment possible, which is determined by the volume/surface ratios of the aerosols and thus depends on their size. The measured d = 70-nm size corresponds to an approximately 6-fold bromine excess, which coincides well with the estimate based on geometric reasoning, showing that the geometric maximal segregation is indeed reached physically. The geometric maximal bromine surface excess for d = 40-nm aerosols (lower dash-dotted line) is lower because of the lower volume/surface ratios compared to the d = 70-nm aerosols. The opposite holds for d = 100-nm aerosols, having a higher maximal surface enrichment than the d = 70-nm aerosols because of their higher volume/surface ratio (upper dash-dotted line), where the larger bulk region acts as a larger reservoir for bromine than in d = 70-nm aerosols. For a macroscopic mixed NaBr/NaCl sample, the high volume/surface ratio implies that the bulk holds enough bromine ions for a high surface enhancement at the surface region since the surface region is small in large samples compared to the bulk. Previously published results on bromine surface segregation in larger systems are also shown in Fig. 4. The surface enhancement reported for bulk NaCl/NaBr mixtures reaches up to 16 times [22] (blue dot) and 35 times [20] (dark green dot). Such a high enrichment is not attainable for nanometer-scale aerosols because of their high surface/volume ratio, and contrary to the present results on nanometer-scale aerosols, large model systems cannot provide realistic values for the surface concentration enhancement for sizes very abundant in the atmosphere.

What drives the Br surface enrichment in the solid aerosols? Two factors are considered: (i) The water/air interface affinity of bromine ions is higher than that of chlorine ions [43,44], and in mixed NaCl/NaBr solutions, Br is surface enhanced at the expense of Cl. This has been observed in bulk water and is assumed to be the case in droplets as well since it is a surface-specific effect and is not expected to vary with the size of the bulk. (ii) The second factor is the different efflorescence points of NaCl and NaBr. As the salt concentration in the droplets increases because of the evaporation of water, it reaches saturation and crystallization will commence. The efflorescence points for NaCl and NaBr are 45% [13] and 23% [45],

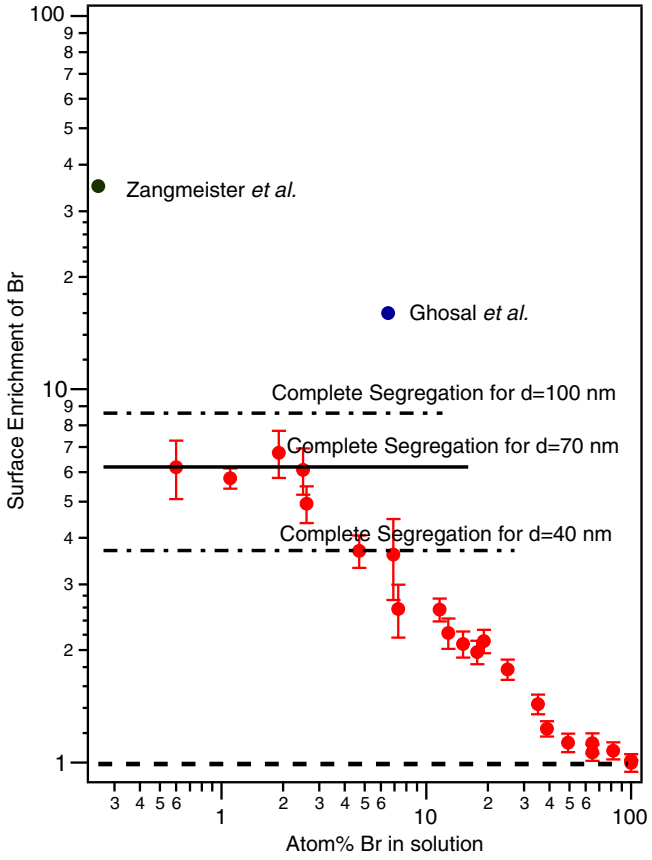

FIG. 4. Surface excess of bromide compared for different NaCl/NaBr mixing ratios in the aqueous droplets. The horizontal full line represents maximal bromide enhancement for complete surface segregation in d = 70-nm solid aerosols. The observed surface enrichment below 2% for d = 70 nm is in good agreement with the value expected for complete segregation. For comparison, the dash-dotted lines indicate the surface enhancement expected for complete bromine segregation in d = 40-nm and d = 100-nm solid aerosols. The bromide surface excesses found by Zangmeister *et al.* [20] and Ghosal *et al.* [22] on larger crystals are also indicated. Because of the very low surface/bulk ratios in large crystals, the bulk serves as a quasi-infinite reservoir of bromide in such extended crystals, allowing higher surface excesses than can be reached in nanometer-scale aerosols. The broken line indicates the bromide surface concentration in the absence of surface segregation.

respectively. For NaCl nanoparticles with diameters larger than 40 nm, the efflorescence point is similar to that of the bulk [13]. For smaller particles, the efflorescence point varies with size because of surface energy effects. The particles used here have an aerodynamic diameter of 70 nm, and size effects are thus not expected to play a role. For sufficiently large droplets, the efflorescence points differ in a similar manner to the molar solubility (6.14 mol/l for NaCl and 8.82 mol/l for NaBr), and segregation in precipitation from mixed (bulk) solutions has been observed, where the chemical composition of the precipitate differs from that of the remaining solution [46,47].

The present findings have crucial implications for atmospheric chemistry involving solid sea-salt aerosols. In the marine boundary layer, where salt-containing droplets are formed by wind action, the high relative humidity prevents their crystallization to solid aerosols. In order for efficient crystallization to occur, transport by wind to regions of lower relative humidity is needed. This can be accomplished by either vertical or horizontal (inland) transport. Under the drying conditions used here, the relative humidity at the outlet of the dryers is 8% and thus significantly below the efflorescence points for both NaCl (45% [13]) and NaBr (23% [45]) and assures a thorough drying. The lack of signal in the O 1s x-ray absorption region provides additional proof for the dryness of solid aerosols. Such dry nanoscopic solid aerosols are not expected in the humid marine boundary layer but are abundant in dryer regions of the atmosphere [48].

The average Br/Cl ratio in sea water is 1:660 (0.15%). This ion ratio lies within the mixing-ratio region where complete bromine surface segregation is observed (Fig. 4). The data in Fig. 2 indicate a maximal bromide surface concentration of 0.95% for the d = 70-nm NaBr/NaCl aerosols with mixing ratios similar to those in sea water. For sea-water samples, the presence of a multitude of other ionic species may complicate the picture, as ionic competition for the aerosol surface will likely not involve only bromine and chlorine, and future studies should address multicomponent mixtures. Nevertheless, since sea-salt aerosols in the atmosphere have a wide size distribution extending from 5 nm to the micron range [14], the present findings indicate that size-dependent surface segregation must be considered in realistic modeling of aerosol chemistry in the atmosphere. As such, the described findings can be considered as a reliable contributor to the key issue of ozone depletion.

IV. CONCLUSIONS

In conclusion, we have measured the local bromine/chlorine surface ratio in solid mixed NaBr/NaCl nanometer-scale aerosols grown from droplets of aqueous solutions. This method mimics the way sea-salt aerosols are generated in the atmosphere from sea spray. We find that surface segregation of bromine takes place. By varying the Br/Cl ratio in the initial droplets, we find that the bromine segregation is complete (all bromine contained in the primary droplets lies in the surface region of the solid aerosol) at Br/Cl mixing ratios below approximately 2%. This finding has potentially far-reaching atmospheric implications since the Br/Cl ratio in sea water is 0.15% and thus within the range where complete surface segregation can take place in nanometer-scale solid aerosols if they are transported away from the marine boundary layer to the region of lower relative humidity where they will crystallize. The level of bromine surface enrichment at complete surface segregation is determined

by the surface/volume ratio of the aerosols, and we demonstrate that macroscopic mixed-salt crystals are not reliable model systems for ion surface segregation in submicron aerosols due to the higher surface/volume ratio of the nanometer-scale aerosols.

ACKNOWLEDGMENTS

The experiments have been performed at the PLEIADES beam line at the SOLEIL Synchrotron, France (Proposal No 20131289). We thank E. Robert for technical assistance, and the SOLEIL staff for stable operation of the equipment and storage ring during the experiments. Professor E. Rühl (FU, Berlin) is warmly acknowledged for inspiring discussions. The aerosol generation and focusing instrumentation used for this work has been funded by the Agence Nationale de la Recherche (ANR) under Grant No. ANR-07-NANO-0031 (Nano-PLEIADES). The authors acknowledge the European COST action CM1204-XUV/X-ray light and fast ions for ultrafast chemistry (XLIC).

[1] V. Masson-Delmotte *et al.*, Information from Paleoclimate Archives, in *Climate Change 2013: The Physical Science Basis. Contribution of Working Group I to the Fifth Assessment Report of the Intergovernmental Panel on Climate Change*, edited by T. F. Stocker *et al.* (Cambridge University Press, Cambridge, England and New York, NY, USA, 2013).

[2] J. Haywood and O. Boucher, *Estimates of the direct and indirect radiative forcing due to tropospheric aerosols: A review*, Rev. Geophys. **38**, 513 (2000).

[3] B. J. Finlayson-Pitts, *The tropospheric chemistry of sea salt: A molecular-level view of the chemistry of NaCl and NaBr*, Chem. Rev. **103**, 4801 (2003).

[4] K. L. Foster, R. A. Plastridge, J. W. Bottenheim, P. B. Shepson, B. J. Finlayson-Pitts, and C. W. Spicer, *The role of* Br_2 *and BrCl in surface ozone destruction at polar sunrise*, Science **291**, 471 (2001).

[5] E. M. Knipping, M. J. Lakin, K. L. Foster, P. Jungwirth, D. J. Tobias, R. B. Gerber, D. Dabdub, and B. J. Finlayson-Pitts, *Experiments and simulations of ion-enhanced interfacial chemistry on aqueous NaCl aerosols*, Science **288**, 301 (2000).

[6] B. J. Finlayson-Pitts and J. C. Hemminger, *Physical chemistry of airborne sea salt particles and their components*, J. Phys. Chem. A **104**, 11463 (2000).

[7] X. Yang, J. A. Pyle, and R. A. Cox, *Sea salt aerosol production and bromine release: role of snow on sea ice*, Geophys. Res. Lett. **35**, L16815 (2008).

[8] X. Yang, J. A. Pyle, R. A. Cox, N. Theys, and M. van Roozendael, *Snow-sourced bromine and its implications for polar tropospheric ozone*, Atmos. Chem. Phys. **10**, 7763 (2008).

[9] R. Vogt, P. J. Crutzen, and R. A. Sander, *Mechanism for halogen release from sea-salt aerosol in the remote marine boundary layer*, Nature (London) **383**, 327 (1996).

[10] S.-M. Fan and D. J. Jacob, *Surface ozone depletion in arctic spring sustained by bromine reactions on aerosols*, Nature (London) **359**, 522 (1992).

[11] *Handbook of Chemistry and Physics*, 74th ed., edited by D. R. Lide (CRC Press, Boca Raton, FL, 1994).

[12] I. N. Tang and H. R. Munkelwitz, *Aerosol phase transformation and growth in the atmosphere*, J. Appl. Meteorol. **33**, 791 (1994).

[13] G. Biskos, A. Malinowski, L. M. Russell, P. R. Buseck, and S. T. Martin, *Nanosize effect on the deliquescence and the efflorescence of sodium chloride particles*, Aerosol Sci. Technol. **40**, 97 (2006).

[14] T. S. Bates, V. N. Kapustin, P. K. Quinn, D. S. Covert, D. J. Coffman, C. Mari, P. A. Durkee, W. J. De Bruyn, and E. S. Saltzman, *Processes controlling the distribution of aerosol particles in the lower marine boundary layer during the first aerosol characterization experiment (Ace 1)*, J. Geophys. Res.: Atmos. **103**, 16369 (1998).

[15] M. Ikegami, K. Okada, Y. Zaizen, and Y. Makino, *Sea-salt particles in the upper tropical troposphere*, Tellus B **46**, 142 (1994).

[16] J. W. Fitzgerald, *Marine aerosols: A review*, Atmos. Environ. **25**, 533 (1991).

[17] P. Jungwirth and D. J. Tobias, *Molecular structures of salt solutions: A new view of the interface with implications for heterogeneous atmospheric chemistry*, J. Phys. Chem. B **105**, 10468 (2001).

[18] S. Ghosal, J. C. Hemminger, H. Bluhm, B. S. Mun, E. L. D. Hebenstreit, Guido Ketteler, D. F. Ogletree, F. G. Requejo, and M. Salmeron, *Electron Spectroscopy of aqueous solution interfaces reveals surface enhancement of halides*, Science **307**, 563 (2005).

[19] B. Winter and M. Faubel, *Photoemission from aqueous solutions*, Chem. Rev. **106**, 1176 (2006).

[20] C. D. Zangmeister, J. A. Turner, and J. E. Pemberton, *Segregation of NaBr in* NaBr/NaCl *crystals grown from aqueous solutions: Implications for sea salt surface chemistry*, Geophys. Res. Lett. **28**, 995 (2001).

[21] T. Koop, A. Kapilashrami, L. T. Molina, and M. J. Molina, *Phase transitions of sea-salt/water mixtures at low temperatures: Implications for ozone chemistry in the polar marine boundary layer*, J. Geophys. Res.: Atmos. **105**, 26393 (2000).

[22] S. Ghosal, A. Shbeeb, and J. C. Hemminger, *Surface segregation in bromide doped NaCl: Implications for the seasonal variations in arctic ozone*, Geophys. Res. Lett. **27**, 1879 (2000).

[23] E. Antonsson, H. Bresch, R. Lewinski, B. Wassermann, T. Leisner, C. Graf, B. Langer, and E. Rühl, *Free Nanoparticles studied by soft x-rays*, Chem. Phys. Lett. **559**, 1 (2013).

[24] A. Lindblad, J. Söderström, C. Nicolas, E. Robert, and C. Miron, *A multi purpose source chamber at the PLEIADES beamline at SOLEIL for spectroscopic studies of isolated species: Cold molecules, clusters, and nanoparticles*, Rev. Sci. Instrum. **84**, 113105 (2013).

[25] P. Liu, P. J. Ziemann, D. B. Kittelson, and P. H. McMurry, *Generating particle beams of controlled dimensions and divergence: I theory of particle motion in aerodynamic lenses and nozzle expansion*, Aerosol Sci. Technol. **22**, 293 (1995).

[26] K. R. Wilson, S. Zou, J. Shu, E. Rühl, S. R. Leone, G. C. Schatz, and M. Ahmed, *Size dependent angular distributions of low-energy photoelectrons emitted from NaCl nanoparticles*, Nano Lett. **7**, 2014 (2007).

[27] J. Meinen, S. Khasminskaya, M. Eritt, T. Leisner, E. Antonsson, B. Langer, and E. Rühl, *Core level photoionization on free sub-10-nm nanoparticles using synchrotron radiation*, Rev. Sci. Instrum. **81**, 085107 (2010).

[28] E. R. Mysak, D. E. Starr, K. R. Wilson, and H. Bluhm, *Note: A combined aerodynamic lens/ambient pressure x-ray photoelectron spectroscopy experiment for the on-stream investigation of aerosol surfaces*, Rev. Sci. Instrum. **81**, 016106 (2010).

[29] *Surface Analysis-The Principal Techniques*, 2nd ed., edited by J. C. Vickerman and I. S. Gilmore (John Wiley & Sons, Chichester, 2009).

[30] C. J. Powell and A. Jablonski, *NIST Electron Inelastic-Mean-Free-Path Database-Version 1.2* (National Institute of Standards and Technology, Gaithersburg, 2010).

[31] See http://www.synchrotron soleil.fr/Recherche/LignesLumiere/PLEIADES.

[32] J. Söderström, A. Lindblad, N. Grum-Grzhimailo, O. Travnikova, C. Nicolas, S. Svensson, and C. Miron, *Angle-resolved electron spectroscopy of the resonant auger decay in xenon with mev energy resolution*, New J. Phys. **13**, 073014 (2011).

[33] O. Travnikova, J.-C. Liu, A. Lindblad, C. Nicolas, J. Söderström, V. Kimberg, F. Gel'mukhanov, and C. Miron, *Circularly Polarized X Rays: Another Probe of Ultrafast Molecular Decay Dynamics*, Phys. Rev. Lett. **105**, 233001 (2010).

[34] C. Miron, C. Nicolas, O. Travnikova, Y.-P. Morin, P. ad Sun, F. Gel'mukhanov, N. Kosugi, and V. Kimberg, *Imaging molecular potentials using ultrahigh-resolution resonant photoemission*, Nat. Phys. **8**, 135 (2012).

[35] V. Kimberg, A. Lindblad, J. Söderström, O. Travnikova, C. Nicolas, Y. P. Sun, F. Gel'mukhanov, N. Kosugi, and C. Miron, *Single-Molecule X-Ray Interferometry: Controlling Coupled Electron-Nuclear Quantum Dynamics And Imaging Molecular Potentials By Ultrahigh-Resolution Resonant Photoemission And Ab Initio Calculations*, Phys. Rev. X **3**, 011017 (2013).

[36] C. Miron, Q. Miao, C. Nicolas, J. D. Bozek, W. Andrałojć, M. Patanen, G. Simões, O. Travnikova, H. Ågren, and F. Gel'mukhanov, *Site-selective photoemission from delocalized valence shells induced by molecular rotation*, Nat. Commun. **5**, 3816 (2014).

[37] M. Patanen, C. Nicolas, X.-J. Liu, O. Travnikova, and C. Miron, *Structural characterization of small xe clusters using their 5s correlation satellite electron spectrum*, Phys. Chem. Chem. Phys. **15**, 10112 (2013).

[38] C. Miron and M. Patanen, *Synchrotron-radiation-based soft x-ray electron spectroscopy applied to structural and chemical characterization of isolated species, from molecules to nanoparticles*, Adv. Mater. **26**, 7911 (2014).

[39] O. Sublemontier, C. Nicolas, D. Aureau, M. Patanen, H. Kintz, X.-J. Liu, M.-A. Gaveau, J.-L. Le Garrec, E. Robert, F.-A. Barreda, A. Etcheberry, C. Reynaud, J. B. A. Mitchell, and C. Miron, *X-ray photoelectron spectroscopy of isolated nanoparticles*, J. Phys. Chem. Lett. **5**, 3399 (2014).

[40] See Supplemental Material at http://link.aps.org/supplemental/10.1103/PhysRevX.5.011025 for the results of x-ray absorption measurements near the O 1s absorption edge.

[41] M. P. Seah and E. D. Hondros, *Grain boundary segregation*, Proc. R. Soc. A **335**, 191 (1973).

[42] S. Brunauer, P. H. Emmett, and E. Teller, *Adsorption of gases in multimolecular layers*, J. Am. Chem. Soc. **60**, 309 (1938).

[43] N. Ottosson, J. Heyda, E. Wernersson, W. Pokapanich, S. Svensson, B. Winter, G. Öhrwall, P. Jungwirth, and O. Björneholm, *The influence of concentration on the molecular surface structure of simple and mixed aqueous electrolytes*, Phys. Chem. Chem. Phys. **12**, 10693 (2010).

[44] S. Ghosal, M. A. Brown, H. Bluhm, M. J. Krisch, M. Salmeron, P. Jungwirth, and J. C. Hemminger, *Ion partitioning at the liquid/vapor interface of a multicomponent alkali halide solution: a model for aqueous sea salt aerosols*, J. Phys. Chem. A **112**, 12378 (2008).

[45] L. Minambres, E. Mendez, M. N. Sanchez, F. Castano, and F. J. Basterretxea, *The effect of low solubility organic acids on the hygroscopicity of sodium halide aerosols*, Atmos. Chem. Phys. **14**, 11409 (2014).

[46] M. G. Siemann and M. Schramm, *Thermodynamic modelling of the br partition between aqueous solutions and halite*, Geochim. Cosmochim. Acta **64**, 1681 (2000).

[47] A. G. Herrmann, *Bromide distribution between halite and nacl-saturated seawater*, Chem. Geol. **28**, 171 (1980).

[48] S. T. Martin, *Phase transitions of aqueous atmospheric particles*, Chem. Rev. **100**, 3403 (2000).